Chinese Chemical Letters 32 (2021) 2503–2508

Contents lists available at ScienceDirect

Chinese Chemical Letters

journal homepage: www.elsevier.com/locate/cclet

Communication

Intercalation modification of FeOCl and its application in dye wastewater treatment

Jiaqiang Wu[a,b], Yanfang Liu[a,b], Xuejing Yang[b,**], Jinling Wang[b], Jie Yang[a,c,*]

[a] School of Energy and Power Engineering, University of Shanghai for Science and Technology, Shanghai 200093, China
[b] School of Mechanical and Power Engineering, East China University of Science and Technology, Shanghai 200237, China
[c] Centre for Environmental Sciences, Hasselt University, Martelarenlaan 42, Hasselt 3500, Belgium

ARTICLE INFO

Article history:
Received 24 September 2020
Received in revised form 20 November 2020
Accepted 9 December 2020
Available online 25 December 2020

Keywords:
FeOCl
Intercalation modification
Coagulation
Dye wastewater treatment
Ion selectivity

ABSTRACT

The textile industry spreads globally with the challenges of its wastewater treatment, especially dyes, which are difficult to degrade. To improve coagulation-flocculation process in dye wastewater treatment, an intercalation process was employed to prepare a new efficient coagulant of lithium borohydride-iron oxychloride ($LiBH_4$_FeOCl) in this study. The layered crystal pristine iron oxychloride (FeOCl) material was prepared by chemical gas phase migration. $LiBH_4$ was introduced into the layers of two dimensional (2D) FeOCl nanosheets by a simple method of liquid phase insertion. The samples were characterized by a field emitting scanning electron microscopy (SEM), a rotating anode X-ray powder diffractometer (XRD), *etc*. The cationic dye was employed as the simulated pollutant. A coagulation and decolorization experimental device was built to study the coagulation performance of the new coagulant $LiBH_4$_FeOCl. It is found that the intercalation modified $LiBH_4$_FeOCl exhibits the characteristics of crystal structure, and the layered structure of FeOCl is preserved. $LiBH_4$_FeOCl, as an insoluble inorganic solid coagulant, performs well for dye pollutants of methyl red, basic yellow 1, methylene blue, rhodamine B, ethyl violet and Janus green B. The reaction rate is significantly 68% higher than the current commercial coagulants of $Al_2(SO_4)_3$. The mechanism analysis reveals that $LiBH_4$_FeOCl breaks and disperses rapidly in the water environment. Its negatively charged material particles can be electrostatically adsorbed with dye pollutant molecules through electrostatic action. The above collaborative actions of breaking, dispersion and electrostatic adsorption are the main coagulation mechanisms of $LiBH_4$_FeOCl. The solid inorganic coagulant of $LiBH_4$_FeOCl provides a competitive alternative for traditional inorganic salts and organic coagulants.

Textile industries positively affect economic development worldwide. It generates around 1 trillion dollars and provides a huge income and employment, particularly for China, The European Union, India and The United States of America. It uses more than 8,000 chemicals to make the 400 billion m^2 of fabric sold annually around the world [1]. Accordingly, 20% of water pollution globally is caused by unacceptable effluent from textile processing, especially synthetic dyes [2]. However, the removal of the color associated with textile dyes has been a great challenge over the past decades. The dyes are non-biodegradable organic compounds. Their high solubility in water makes it difficult for removal [3].

In recent years, physical, chemical and biological methods have been studied to remove the color from textile effluents. But these methods still have problems of high cost, inadequate efficiency, extra pollution, *etc.* For example, adsorbents in physical methods are usually difficult to regenerate. Chemical methods of oxidation come with extra pollution. Synthetic dyes have a harmful effect on the organisms used in biological methods [4–6].

The coagulation-flocculation process is the most widely used in wastewater treatment due to its simplicity and cost-effectiveness. In this process, suspended and colloidal particles are destabilized, using coagulant agents, and gather together to form large agglomerates. These agglomerates can be separated by gravity settling [7]. Aluminum sulfate is the most commonly used in wastewater treatment processes. The coagulants of iron salts and polyaluminum chloride (PACl) were reported as well [8].

* Corresponding author at: Centre for Environmental Sciences, Hasselt University, Martelarenlaan 42, Hasselt 3500, Belgium.
** Corresponding author.
E-mail addresses: xj.yang@ecust.edu.cn (X. Yang), jie.yang@uhasselt.be, wdpz_ygpz@163.com (J. Yang).

https://doi.org/10.1016/j.cclet.2020.12.043
1001-8417/

Verma *et al.* [9] studied the effect of different coagulants on the quality of effluent from sewage treatment. The results showed that under the condition of pH 5.6 and the dosage of $FeCl_3$ was 3,000 mg/L, the chemical oxygen demand (COD) removal rate 75.5%. In addition, in the study of sludge sedimentation and filtration characteristics, it was found that the use of cationic polyacrylamide (concentration of 175 mg/L) and ferric chloride at the same time improved the filtration performance and reduced the specific resistance of filter cake. Harrelkas *et al.* [10] applied the combination of physical and chemical treatment to the actual textile wastewater samples. The experimental results showed that the optimal process parameters were pH 5, coagulant ($Al_2(SO_4)_3$) 100 mg/L and flocculants 4 mg/L. The turbidity removal rate was about 60%, and the COD removal rate was not more than 20%. Chu *et al.* [11] used alum to treat printing and dyeing wastewater and reduced the consumption of 1/3 fresh alum per month. However, due to the high solubility of hydrophilic dyes, the water quality may decline during the backwater period, so the process cannot be used for the removal of hydrophilic dye wastewater. Yang *et al.* [12] used $Al_2(SO_4)_3$ and polyaluminium chloride (PAC) to study the coagulation performance and residual aluminum form in Yellow River water. The results showed that the best treatment was pH 6.0. In most cases, PAC showed better coagulation performance than $Al_2(SO_4)_3$. For example, at a dosage of 15 mg/L, PAC achieved an optimum removal efficiency of turbidity, UV_{254} and DOC of 96.3%, 57.1% and 32.7%, respectively, and $Al_2(SO_4)_3$ also achieved an optimum removal efficiency of turbidity, UV_{254} and DOC of 94.5%, 53.5% and 34.8%, respectively.

Although these coagulants have been widely used and studied, they have disadvantages of sensitivity to sample specific characteristics, insufficient charge neutralization, and so on. More research is needed to further improve the properties of the coagulants and focus on understanding the behavior and aquatic chemistry of the coagulants.

To improve the performances of coagulation-flocculation process in dye wastewater treatment, an intercalation process was employed to prepare a new efficient coagulant of lithium borohydride-iron oxychloride ($LiBH_4$_FeOCl) in this study. The intercalation process in chemistry is the reversible inclusion or insertion of a molecule (or ion) into compounds with layered structures. It combines solid materials of different structural dimensionality with atomic or molecular guest species to design the solids with particular composition, structure and physical properties [13]. This research intercalated lithium borohydride ($LiBH_4$) as the guest species into the layers of two dimensional (2D) iron oxychloride (FeOCl) nanosheets. FeOCl, possessing a layered 2D nanosheet structure, has high structure-dependent activity [14]. $LiBH_4$ was selected as the intercalation species to enhance the activity of FeOCl. Because $LiBH_4$ is a relatively mild reducing agent, which hydrolyzes in the solution to split the FeOCl layers. It increases the reaction area of FeOCl. Meanwhile, the mild hydrolysis reaction of $LiBH_4$ will not break the FeOCl layers. In this study, the intercalation compound of $LiBH_4$_FeOCl was prepared with a liquid phase intercalation method by dispersing $LiBH_4$ and FeOCl in tetrahydrofuran solution, and then mixing the two dispersing systems. So that $LiBH_4$ was introduced into the FeOCl interlayer. The samples were analyzed by SEM, XRD, FT-IR, *etc.* The cationic dye was employed as the simulated pollutant. A coagulation and decolorization experimental device was built to study the coagulation performance of the new coagulant $LiBH_4$_FeOCl.

FeOCl in the pure phase was prepared by a chemical vapor migration method [15]. The insertion of $LiBH_4$ refers to Weber's method and has been improved [16]. The typical operation is as follows: in the glove box at room temperature and argon atmosphere, weigh 125 mg (1.165 mmol) of FeOCl, dissolve it and disperse it in the quartz glass tube with 5.89 mL tetrahydrofuran (THF) seal mouth, add 0.115 mL $LiBH_4$ (2 mol/L in THF, 0.466 mmol), mix them and stir for 12 h. The above products were washed with THF several times in an argon atmosphere to remove the unreacted $LiBH_4$. The washed products were dried in vacuum overnight and transferred to the glove box for preservation.

An experimental device was built (Fig. S1 in Supporting information), using the jacketed bottle device and constant temperature water bath to control the experimental temperature. The specific operation was: Take 50 mL of dye wastewater containing 25 mg/L of simulated dye concentration and adjust the pH of the experimental solution to be adjusted by HNO_3 solution and NaOH solution, respectively. The coagulant $LiBH_4$_FeOCl was weighed according to the dosage of 200 mg/L. The coagulant was added into the simulated dye wastewater at the beginning of the coagulation process. After it had started reaction for a certain time, the samples were collected through a polytetrafluoroethylene (PTFE) membrane with a pore size of 0.22 μm. The dye concentration in the filtrate was tested by spectrophotometry. COD was determined by rapid digestion.

Firstly, the phase changes of FeOCl before and after intercalation were analyzed by XRD. As shown in Fig. 1a, the XRD peak of pure FeOCl is completely consistent with that of its PDF standard card (PDF-JCPDS No. 39-0612), which is mainly located at the positions of 2θ 11.18°, 26.09°, 35.31°, 45.76° and 50.40°, respectively corresponding to (010), (110), (021), (111), (031) crystal plane. The typical (010) crystal surface characteristic peak position of FeOCl after intercalation moved from 11.18° to 7.32° in low angle, which indicated that the interlayer spacing expanded about 4.16 Å (from 7.94 Å to 12.10 Å). At the same time, the derived peak intensity of the intercalated material is lower than that of the original FeOCl, accompanied by the broadening of the diffraction peak. It can be observed by SEM (Figs. 1b and c) that intercalation makes FeOCl expand in the direction of the extended layer structure, and the regularity of its particles is lower than that of the original FeOCl. Based on the characterization, the intercalation of

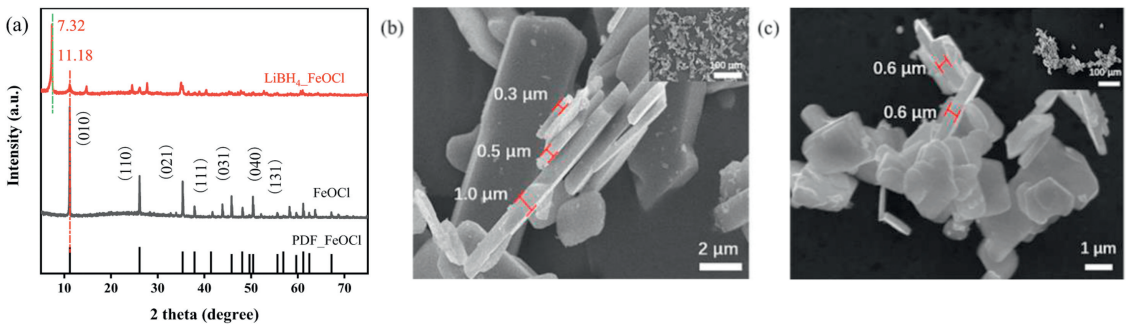

Fig. 1. XRD spectra of $LiBH_4$_FeOCl and FeOCl and its powder diffraction crystal library (a). SEM image of FeOCl (b). SEM image of $LiBH_4$_FeOCl (c).

$LiBH_4$ makes the FeOCl layer spacing expand, which makes it is more likely to peel and break due to the weakening of the van der Waals force between layers. And those changes may be conducive to its diffusion in the water environment.

Furthermore, the valence changes of FeOCl before and after the intercalation were characterized by a X-ray photoelectron spectroscopy (XPS). Compared with the original FeOCl, the intercalated material has an obvious B 1s signal (as shown in Fig. 2a). Combining with the XRD results, it can be concluded that $LiBH_4$ is successfully introduced into the interlayer of FeOCl through intercalation reaction. It is generally believed that the intercalation reaction between the host and guest of FeOCl accompanies the charge transfer between them, that is, the reduction of FeOCl and the oxidation of the guest. Tsai *et al.* [17] have studied the reduction of the intercalated $LiBH_4$ compound, and believe that the oxidation products are B_2H_6 and H_2. Based on this understanding, we think that the redox reaction of intercalated FeOCl can be described as follows (Reaction 1).

$$LiBH_4 + FeOCl \leftarrow Li_xFeOCl + B_2H_6 + H_2\uparrow \quad (1)$$

In the process of material preparation, an obvious bubble release was observed, which confirmed the formation of hydrogen. Fig. 2b shows the change of Fe $2p_{3/2}$ peak of the material before and after intercalation. It can be found that there is an obvious shoulder peak at ~708 eV in $LiBH_4$_FeOCl, which also proves that Li^+ embedment causes the reduction of Fe(III) to Fe(II) in the FeOCl skeleton. Therefore, it can be considered that the reduction of FeOCl and the oxidation of $LiBH_4$ occurred in the process of FeOCl intercalation. Li^+ is introduced into the interlayer of FeOCl as a structural intercalation guest, while B_2H_6 exists in the interlayer of FeOCl as a co intercalation species. Due to the strong reducibility of B_2H_6 in aqueous solution, further structural evolution of the material may be induced, which will directly affect the charge performance of the material.

At first, rhodamine B (RhB) was used as a model dye pollutant to investigate the coagulation effect of $LiBH_4$_FeOCl. At the initial stage of adding $LiBH_4$_FeOCl, it was observed that there are microbubbles in the solution, which may be caused by the reaction of residual $LiBH_4$ between layers and water. The color and COD removal rates as functions of reaction time is shown in Fig. 2c. It can be found that the majority of RhB can be removed within 2 min after $LiBH_4$_FeOCl was added. With the increase of reaction time, the removal rate increases gradually, and the removal ratio (after 30 min) is close to 100%. The trend of the COD removal ratio is the same as that of the decolorization ratio.

Our group reported the generation mechanism of hydroxyl radicals from FeOCl and H_2O_2, and found the combination of FeOCl and oxidant H_2O_2 could remove 100% of organics from trace organic wastewaters [15]. The application of oxidation reaction in the treatment of dye wastewater generally shows that the generated hydroxyl radicals attack the dye chromogenic groups to break their chemical bonds off. The dye macromolecules first degrade into smaller molecules, then the continuously produced ·OH attacks these small molecules to mineralize them into CO_2 and H_2O. In this process, although it shows a high decolorization rate at the beginning of the reaction, the COD value decreases slowly first, then goes down fast. However, in our experimental system, the changing trend of COD in Fig. 2c is consistent with the change of decolorization rate, both of which show a rapid decrease at the beginning, and then a mild change. Furthermore, the LC–MS/MS tests indicated that none of the intermediate products from the possible pathway of RhB oxidative degradation was detected. It shows the oxidative degradation does not get involved in this decolorization system with $LiBH_4$_FeOCl.

Furthermore, the dye pollutants that expanded from RhB to the other ten different dyes present similar characteristics in Fig. 2d (Table S1 in Supporting information shows the structure and additional information). It can be found that $LiBH_4$_FeOCl has apparent charge selectivity for the coagulation effect of these dyes. As shown in Fig. 2e, FeOCl has very limited color removal abilities for these dyes. But it shows an excellent decolorization performance for the $LiBH_4$_FeOCl system of basic cation and neutral dye. The removal ratio reaches above 95% after 30 min of reaction, but the system has no obvious removal for acid anion dye. This charge selectivity may be related to the charging behavior of the material in water, which will be analyzed in detail in the part of the coagulation mechanism.

In order to exclude the possible influence of other species, we have investigated the removal of RhB when $LiBH_4$, $NaBH_4$, $Fe(OH)_3$, LiCl and FeOCl are added, respectively. As shown in Fig. 2f, $Fe(OH)_3$,

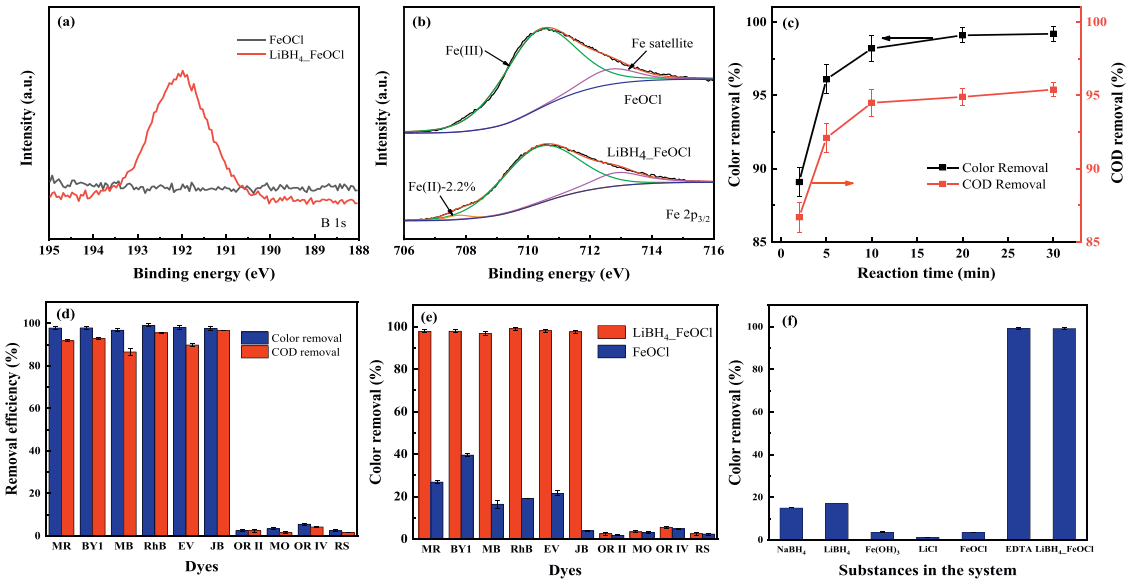

Fig. 2. XPS spectra of FeOCl and $LiBH_4$_FeOCl B 1s (a) and Fe $2p_{3/2}$ (b). The color and COD removal rates of $LiBH_4$_FeOCl as functions of reaction time (c). The color and COD removal rates of $LiBH_4$_FeOCl on different dyes (d). Decolorization effects of FeOCl and $LiBH_4$_FeOCl on different dyes (e). Decolorization effects of different substances on RhB in the system (f).

LiCl and FeOCl had almost no decolorization effect on RhB, while $LiBH_4$ and $NaBH_4$ had a certain decolorization effect on RhB, which may be caused by their reducibility, but their decolorization rate (~20%) was far less than $LiBH_4$_FeOCl. In addition, taking into account the effects of iron ion leaching in the sample, add the appropriate amount of ethylene diamine tetraacetic acid (EDTA) sodium to the dye before adding it. The experimental results show that the addition of EDTA has little effect on the coagulation and decolorization of $LiBH_4$_FeOCl. The above results exclude the effect of other species on RhB decolorization and prove that the unique structure of $LiBH_4$_FeOCl is the main reason of RhB decolorization.

In order to analyze the mechanism of $LiBH_4$_FeOCl decolorizing dye RhB wastewater, the reaction solution was filtered and detected by a ultraperformance liquid chromatography-tandem mass spectrometry (UPLC-MS/MS) when the reaction was carried out for 5 min. The UPLC-MS signal is shown in Fig. 3a, and three substance peaks can be found in the spectrum, and their retention times are 3.93, 4.10 and 4.89 min, respectively. Additionally, the mass spectrum of these three peaks shows that the strongest mass charge ratios at the peak positions are 149.02, 193.12 and 279.16, respectively, which are different from the possible degradation intermediates of RhB (Table S2 in Supporting Information shows RhB and its Fenton degradation intermediate structure and *m/z* ratio information). Therefore, the contribution of oxidative degradation to the removal of RhB can be excluded, which proves that the removal of RhB is the decolorization caused by coagulation adsorption.

We also used a fourier transform infrared spectrometry (FT-IR) to characterize the chemical bonds and functional groups of the $LiBH_4$_FeOCl after intercalation reaction in aqueous solution, and further analyze the coagulation mechanism of $LiBH_4$_FeOCl. As shown in Figs. 3b–d, compared with the original FeOCl, the infrared spectrum Fe-O vibration of $LiBH_4$_FeOCl after modification is slightly red-shifted compared with FeOCl. A new peak appears at 412 cm^{-1}, accompanied by the weakening of the absorption peak intensity of the Fe-O vibration at 486 cm^{-1}, indicating the decline of the Fe-O bond [18]. The infrared spectrum of $LiBH_4$_FeOCl at 1620 ± 10 cm^{-1} shows a slight blue shift of the water variable angle, a vibration peak, and the strength is enhanced. It indicates that the modified material has a stronger ability to absorb water, and the O—H bond energy is enhanced [19]. A new weak absorption peak appeared at 1297 cm^{-1} and 1388 cm^{-1} in the infrared spectrum of $LiBH_4$_FeOCl, which was mainly caused by the asymmetric stretching vibration of the Fe−OH-Fe group formed in $LiBH_4$_FeOCl. It indicates that the surrounding environment of Fe in $LiBH_4$_FeOCl had changed, which was conducive to the absorption bridging polymerization of coagulants, and thus showed better coagulation performance.

In the study of activity, it has been found that $LiBH_4$_FeOCl has obvious charge selectivity for dye coagulation. This charge selectivity indicates that the coagulation of dye molecules by $LiBH_4$_FeOCl is likely to be realized through the adsorption of charge interaction. In order to explore the relationship between the surface charge and the mechanism of coagulation and decolorization, we analyzed the zeta potential value of $LiBH_4$_FeOCl after it was directly added into water. It has a negative charge property in deionized water with a charge value of 32.4 mV. Its absolute value is higher than FeOCl of −30.32 mV, reported by Zhang *et al.* [20]. It can be inferred that the surface charge of the material is negatively charged due to the deblocking of Li^+ after the expansion of $LiBH_4$_FeOCl in a water environment. This shows that under the condition of direct addition, $LiBH_4$_FeOCl can absorb basic cations and neutral dyes through electrostatic action. In order to further demonstrate the charge selectivity of coagulation activity, we have investigated RhB decolorization activity under different pH (Fig. S2 in the Supporting information). It exhibits that with the increase of pH value, the decolorization rate of RhB decreases gradually. It can be caused by the increase in the concentration of OH^- in aqueous solution as a cationic dye, and the action of OH^- with RhB to neutralize its charge, resulting in a decrease of the decolorization rate of RhB at alkaline pH. The dosage and reaction time were adjusted to study the coagulation ability of $LiBH_4$_FeOCl under different acidities. The kinetic study of color removal efficiency of different dosages of coagulant (Fig. S3a in the Supporting information) shows that the color removal efficiency rises with the increase of coagulant dosage. When the dosage of coagulant increases to 200 mg/L, the decolorization rate is stable at about 100%. The color removal efficiency increases with the reaction time (Fig. S3b in the Supporting information). The lower the pH value is, the higher the coagulation rate gets. This is caused by the negative

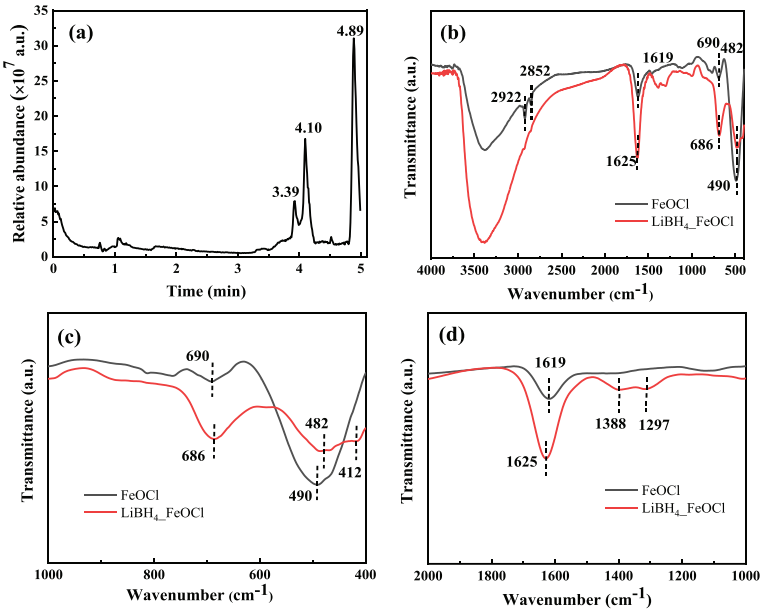

Fig. 3. (a) UPLC-MS/MS spectra of RhB by coagulation experiment. (b) FTIR spectra of FeOCl and $LiBH_4$_FeOCl in wavenumber range from 400 cm^{-1} to 4000 cm^{-1}. (c) An enlarged view at 400 cm^{-1} to 4000 cm^{-1} of (b). (d) An enlarged view at 1000 cm^{-1} to 2000 cm^{-1} of (b).

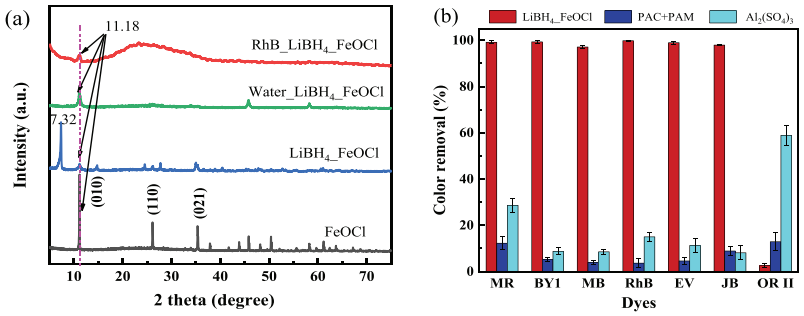

Fig. 4. (a) XRD spectra of different materials. (b) Decolorization effects of $LiBH_4$_FeOCl and the conventional coagulants of PAC and $Al_2(SO_4)_3$ on different dyes.

charge on the coagulant's surface and the electrostatic interaction with the cations in the solution.

The aqueous RhB_$LiBH_4$_FeOCl system was also analyzed by XRD in this study, shown in Fig. 4a. It indicates the red curve of RhB_$LiBH_4$_FeOCl is rough and burr. It means the $LiBH_4$_FeOCl material has lost its crystal structure characteristics. The flocs are formed after the RhB_$LiBH_4$_FeOCl system is decolored. The system does not retain the crystal structure of the raw material anymore. According to the Fenton-like reaction [15], the crystal structure of the material does not change before and after the redox reaction with FeOCl as a catalyst. It demonstrates $LiBH_4$_FeOCl does not perform as a Fenton-like reagent in the decolorization process of this study.

The above electrostatic adsorption process was also confirmed by SEM analysis (Fig. S4a in Supporting information). After filtering and drying the flocs, SEM characterization shows that the flocs are piled up by many single or several layers of flakes, and there are a large number of small particles attached to the surface gap of the flocs. The reason is that the dye molecules lose stability in water due to the surface charge of the materials, and are adsorbed by electrostatic. The surface of the modified material $LiBH_4$_FeOCl, while the petal-like structure of the hydrated $LiBH_4$_FeOCl enhanced its electrostatic adsorption and bridging ability. According to the EDS energy spectrum analysis of small particles on the floc surface and layered material substrate (the results are shown in Figs. S4b and c in Supporting information). It reveals that the N element content of small particles is much higher than that in other areas. According to the chemical formula of dye RhB, it is speculated that it is the crystal particles that are precipitated by polymerization and precipitation of RhB dye on the floc surface after drying.

To sum up, the coagulation mechanism of $LiBH_4$_FeOCl on dye molecules is, through the intercalation of $LiBH_4$ in FeOCl, structural object species Li^+ and intercalation species B_2H_6 is introduced between FeOCl layers. This intercalation process makes the layered structure of FeOCl change, peeling and breaking. At the same time, the abnormal change of the Fe coordination field structure tends to induce the formation of coordination unsaturated sites on the surface of the material, which makes the charge properties change. In the water environment, the interaction of B_2H_6 and water will generate hydrogen, which will promote the expansion and fracture of the layered structure. This process makes $LiBH_4$_FeOCl expand rapidly in the water. The surface of the expanded material is negatively charged due to the desorption of Li^+ species, and the adsorption and removal of alkali cations and neutral dyes can be made through electrostatic action.

In addition, we have compared the $LiBH_4$_FeOCl with traditional coagulants PAC and $Al_2(SO_4)_3$ in dye removal (Fig. 4b). The results show that the coagulation and decolorization effects of $LiBH_4$_FeOCl are much better than that of traditional coagulants within 30 min. The $LiBH_4$_FeOCl is able to decolorize dye wastewater efficiently.

To improve coagulation-flocculation process in dye wastewater treatment, a new efficient coagulant of $LiBH_4$_FeOCl was prepared and characterized in this study. $LiBH_4$ was intercalated into the layers of 2D FeOCl nanosheets to enhance the catalytic activity of FeOCl. A coagulation and decolorization experimental device has been built to study the coagulation performance of the new coagulant $LiBH_4$_FeOCl. The results show that the intercalation modified $LiBH_4$_FeOCl exhibits the characteristics of crystal structure, and the layered structure of FeOCl is preserved. The study of the coagulation mechanism reveals that the interstitial object of the $LiBH_4$ can induce the change of $LiBH_4$_FeOCl structure and charge properties in aquatic environments. It enhances the adsorption of a dye molecule by the electric charge effect. $LiBH_4$_FeOCl, as an insoluble inorganic solid material, has excellent coagulation performance for dye pollutants of methyl red, basic yellow 1, methylene blue, rhodamine b, ethyl violet and Janus green B. The reaction rate is 68% higher than the current commercial coagulants of $Al_2(SO_4)_3$. The mechanism analysis reveals that $LiBH_4$_FeOCl breaks and disperses rapidly in the water environment, and its negatively charged material particles can be electrostatically adsorbed with dye pollutant molecules through electrostatic action. The above collaborative actions of breaking, dispersion and electrostatic adsorption are the main coagulation activities of $LiBH_4$_FeOCl. As an inorganic solid material, the successful development of the $LiBH_4$_FeOCl coagulation system provides a competitive alternative route in dyes wastewater treatment.

Declaration of competing interest

The authors report no declarations of competing interest.

Acknowledgments

The authors gratefully acknowledge the financial supports by the National Key Basic Research Program of China (No. 2019YFC1906700), National Natural Science Foundation of China (Nos. 21876049, 51878643) and University of Shanghai for Science and Technology (Grant Agreement No. ZR18PY01).

Appendix A. Supplementary data

Supplementary material related to this article can be found, in the online version, at doi:https://doi.org/10.1016/j.cclet.2020.12.043.

References

[1] B. Lellis, C.Z. Fávaro-Polonio, J.A. Pamphile, J.C. Polonio, Biotechnol. Res. Innov. 3 (2019) 275–290.
[2] S.C. Bhatia, S. Devraj, Pollution Control in Textile Industry, WPI India, 2017.
[3] D.P. Mohapatra, M. Cledón, S.K. Brar, R.Y. Surampalli, Water Air Soil Pollut. 227 (2016) 77–91.

[4] S. Arslan, M. Eyvaz, E. Gürbulak, E. Yüksel, A review of state-of-the-art technologies in dye-containing wastewater treatment-the textile industry case, in: E.P.A. Kumbasar, A.E. Körlü (Eds.), Textile Wastewater Treatment, IntechOpen, London, 2016, pp. 1–28.
[5] M. Ghorbani, H. Eisazadeh, Compos. Part B 45 (2013) 1–7.
[6] L. Szpyrkowicz, C. Juzzolino, S.N. Kaul, Water Res. 35 (2001) 2129–2136.
[7] N.D. Tzoupanos, A.I. Zouboulis, 6th IASME/WSEAS International Conference on Heat Transfer, Rhodes, Greece, 2008.
[8] P. Pourrezaei, P. Drzewicz, Y. Wang, et al., Environ. Sci. Technol. 45 (2011) 8452–8459.
[9] S. Verma, B. Prasad, I.M. Mishra, J. Hazardous Mater. 178 (2010) 1055–1064.
[10] F. Harrelkas, A. Azizi, A. Yaacoubi, A. Benhammou, M.N. Pons, Desalination 235 (2009) 330–339.
[11] W. Chu, Water Res. 35 (2001) 3147–3152.
[12] Z. Yang, B. Gao, Q. Yue, Chem. Eng. J. 165 (2010) 122–132.
[13] W. Müller-Warmuth, R. Schöllhorn, Progress in Intercalation Research, Springer, United States, 2012.
[14] J. Luo, M. Sun, C.L. Ritt, et al., Environ. Sci. Technol. 53 (2019) 2075–2085.
[15] X. Yang, X. Xu, J. Xu, Y. Han, J. Am. Chem. Soc. 135 (2013) 16058–16061.
[16] D. Weber, L.M. Schoop, V. Duppel, et al., Nano Lett. 16 (2016) 3578–3584.
[17] H. Tsai, J. Heising, J.L. Schindler, C.R. Kannewurf, M.G. Kanatzidis, Chem. Mater. 9 (1997) 879–882.
[18] I.V. Chernyshova, M.F. Hochella Jr, A.S. Madden, Phys. Chem. 9 (2007) 1736–1750.
[19] W. Chen, H. Zheng, J. Zhai, et al., Spectrosc. Spect. Anal. 36 (2016) 1038–1043.
[20] J. Zhang, G. Liu, S. Liu, New J. Chem. 42 (2018) 6896–6902.